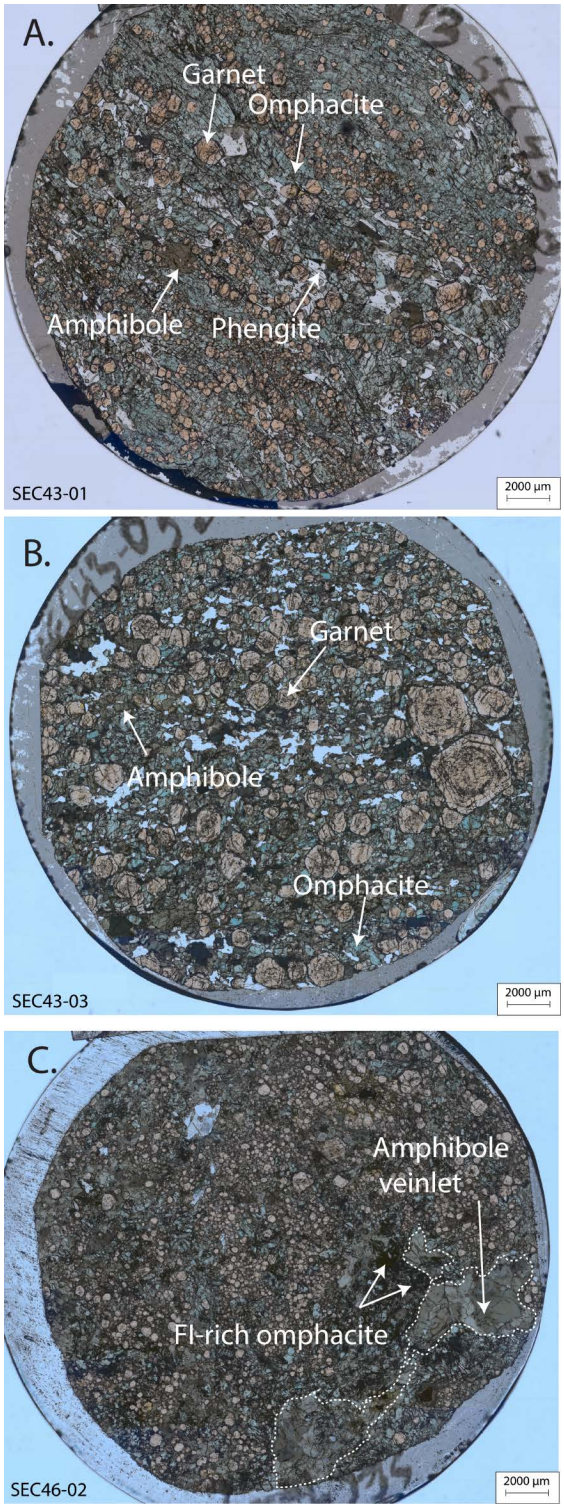

Supplemental Figure S1. Representative full-section photomicrographs of Raspas samples analyzed in this study. (**a**) Prograde assemblage in SEC43-01 contains garnet porphyroblasts within a matrix of omphacite and lesser quartz and phengite with minor apatite and rutile. The sample shows no evidence for retrogression. (**b**) SEC43-03 megacrystic garnet showing sector zoning with minor quartz. (**c**) Amphibole veinlet in sample SEC46-02, outlined in white dashed line. Adjacent omphacite shows abundant fluid inclusions (dark patches).

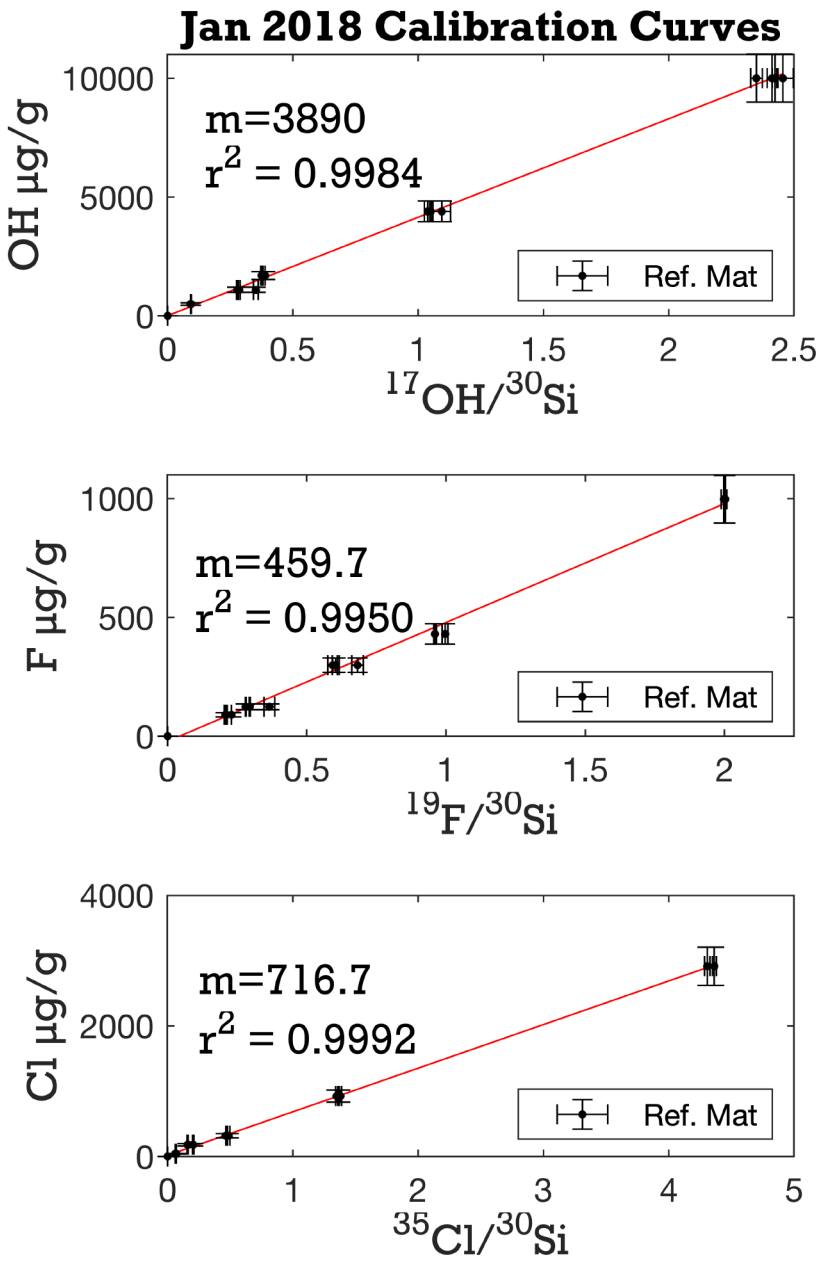

Supplemental Figure S2. Representative calibration slope used in this study. Calibration slope confidence intervals were calculated with a nonlinear bootstrapping technique using 5000 iterations.

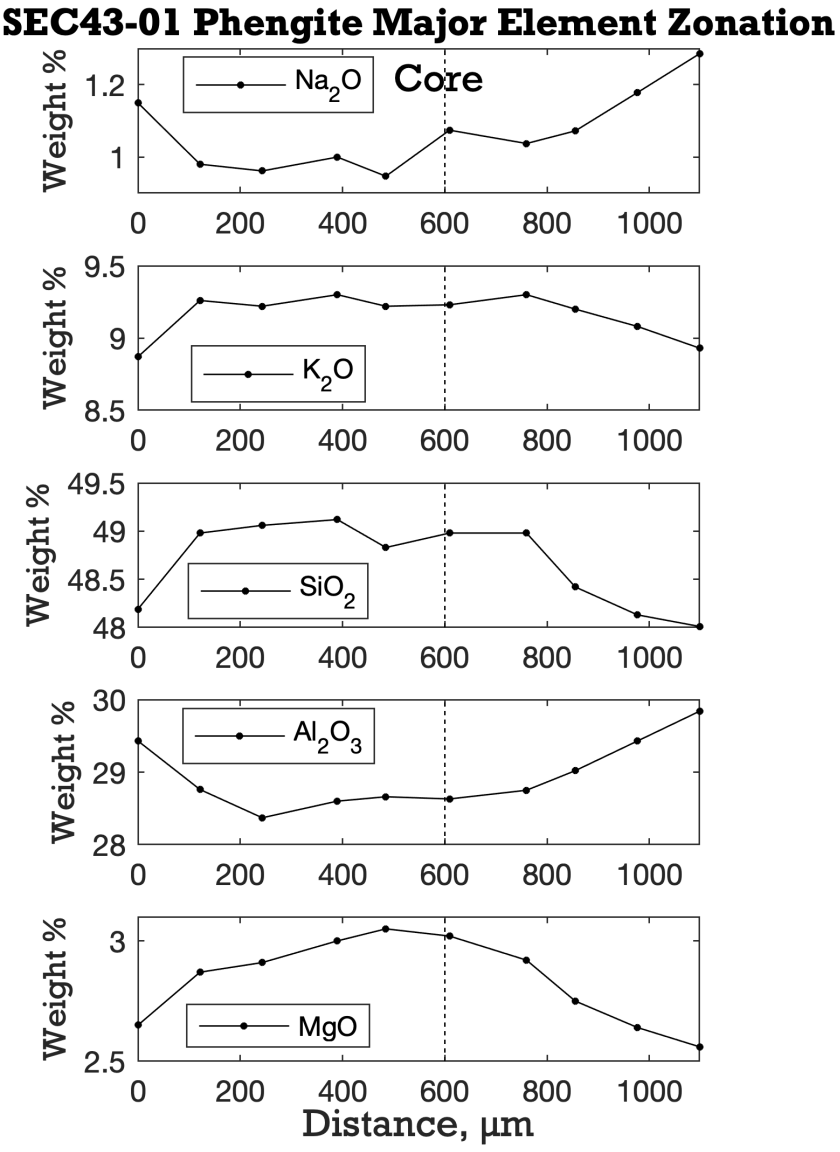

Supplemental Figure S3. SEC43-01 phengite EMP profile from rim to rim shows Na_2O and Al_2O_3 increases from core to rim, while K_2O, SiO_2, and MgO all decrease toward the grain boundary.

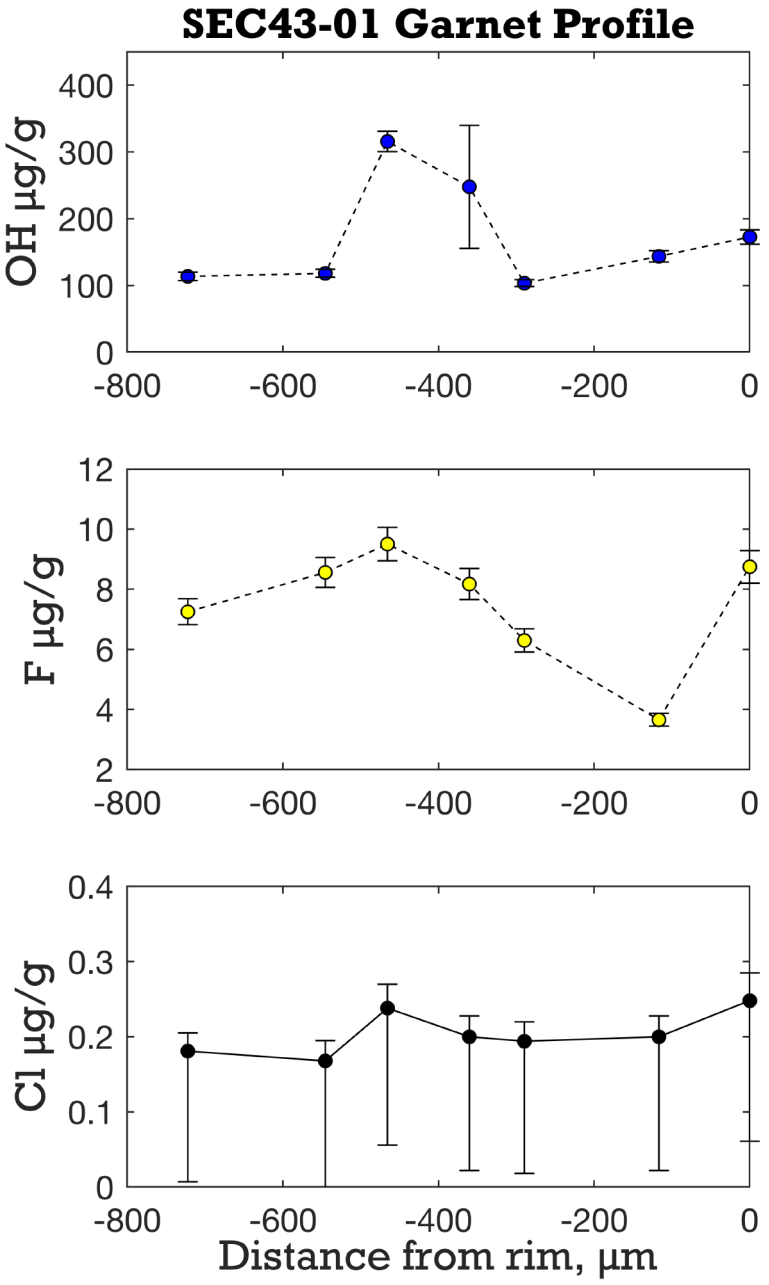

Supplemental Figure S4. SEC43-01 garnet core to rim transect. Zero values represent rim, 750 µm spot location is the garnet core. Overall, OH and F show intragrain variability likely related to partitioning and re-equilibration during garnet growth. The combination of internal and propagated calibration slope uncertainty corresponds to the positive error bar on our analyses. The negative error bars are larger for Cl because they incorporate the conservative uncertainty on the maximum background.

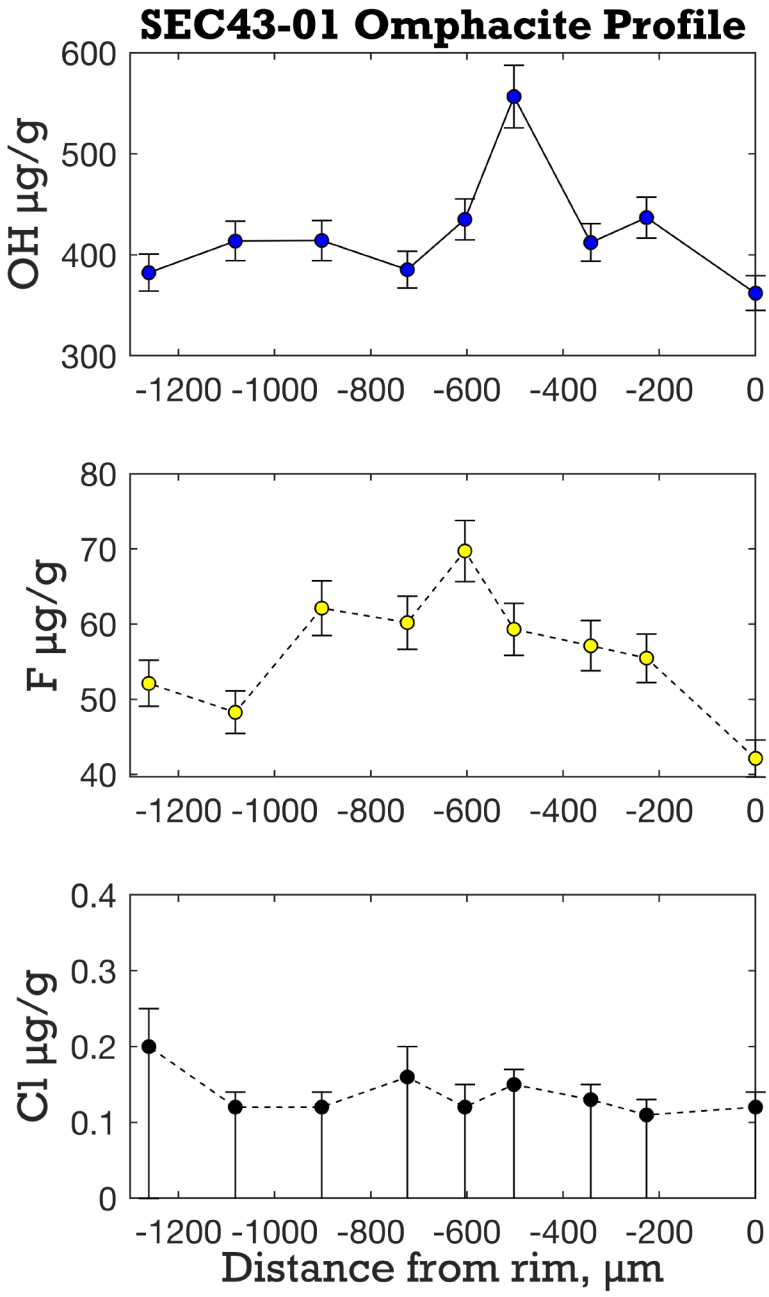

Supplemental Figure S5. SEC43-01 omphacite core (~1300 µm) to rim (0 µm) profile for OH, F, and Cl. Significant variations occur on length scales of <100 µm, with apparent rim depletions in F and OH.

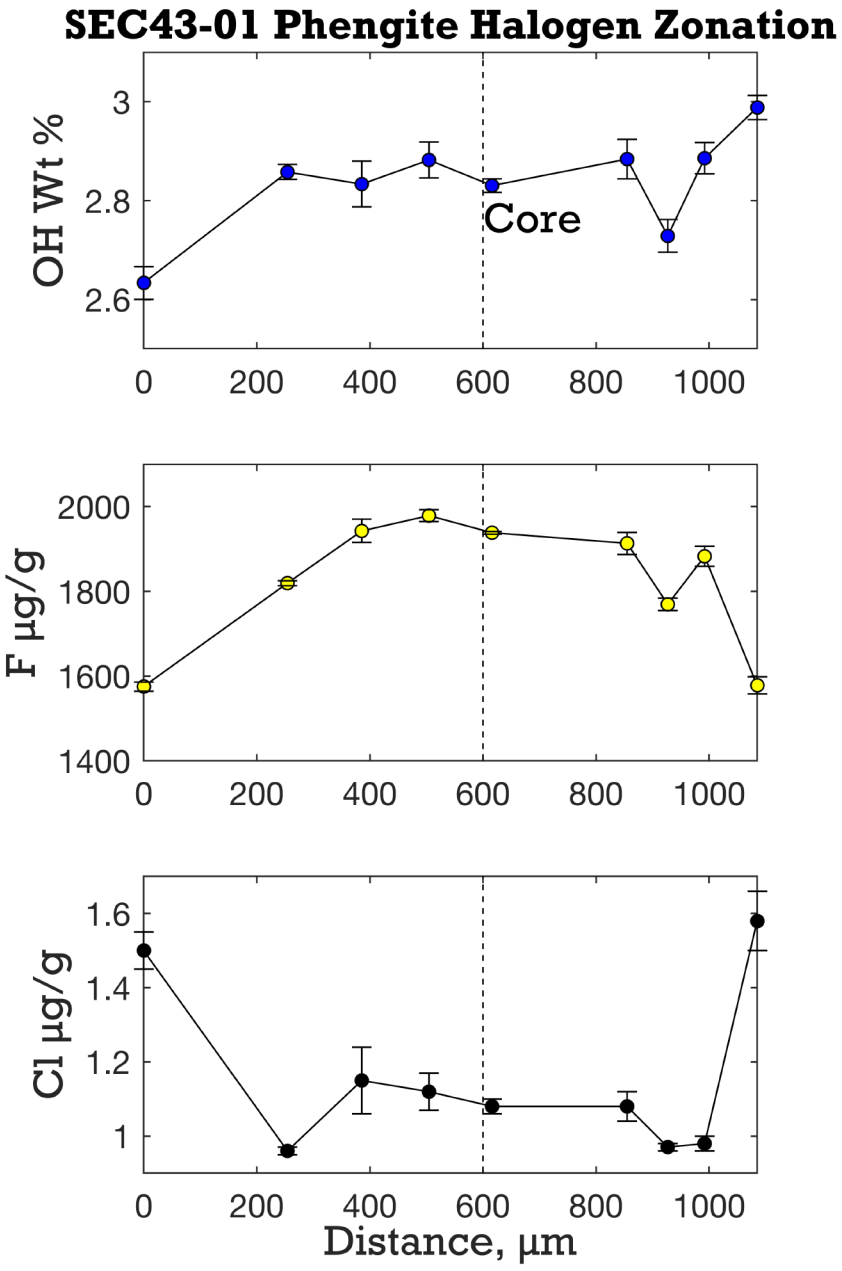

Supplemental Figure S6. SEC43-01 phengite rim-to-rim transect. F shows depletions toward the grain boundaries, while Cl shows rim enrichments of approximately 40%.

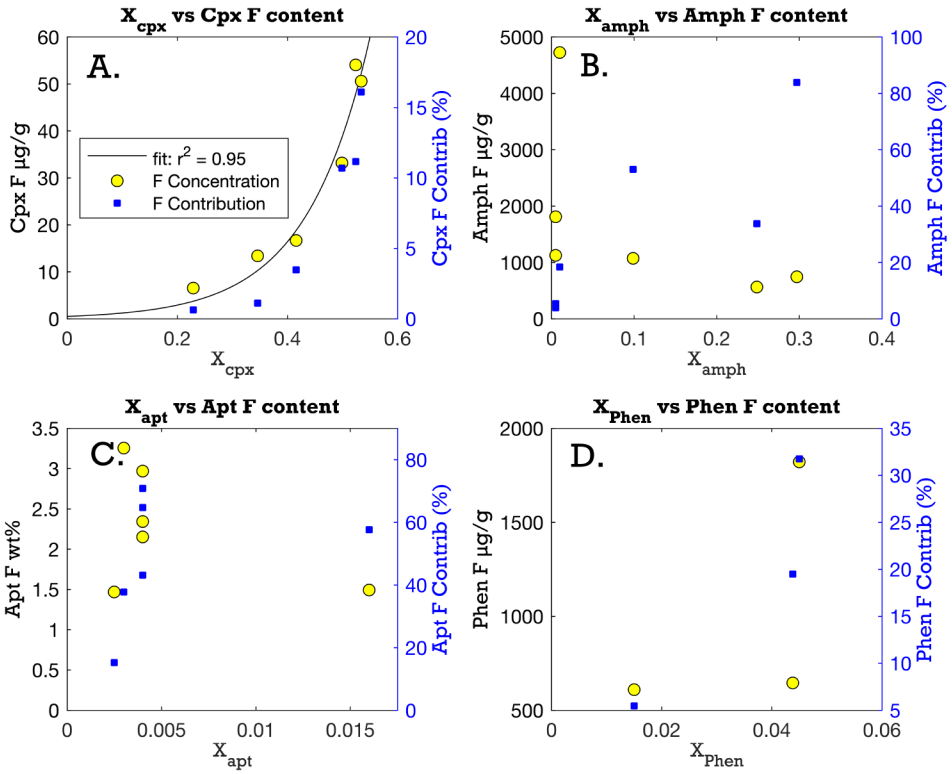

Supplemental Figure S7. Fluorine concentrations (black y-axis, yellow dots) and contributions to the bulk-rock (blue y-axis, blue dots) plotted against modal proportion of each phase for (**a**) omphacite, (**b**) amphibole, (**c**) apatite, and (**d**) phengite.

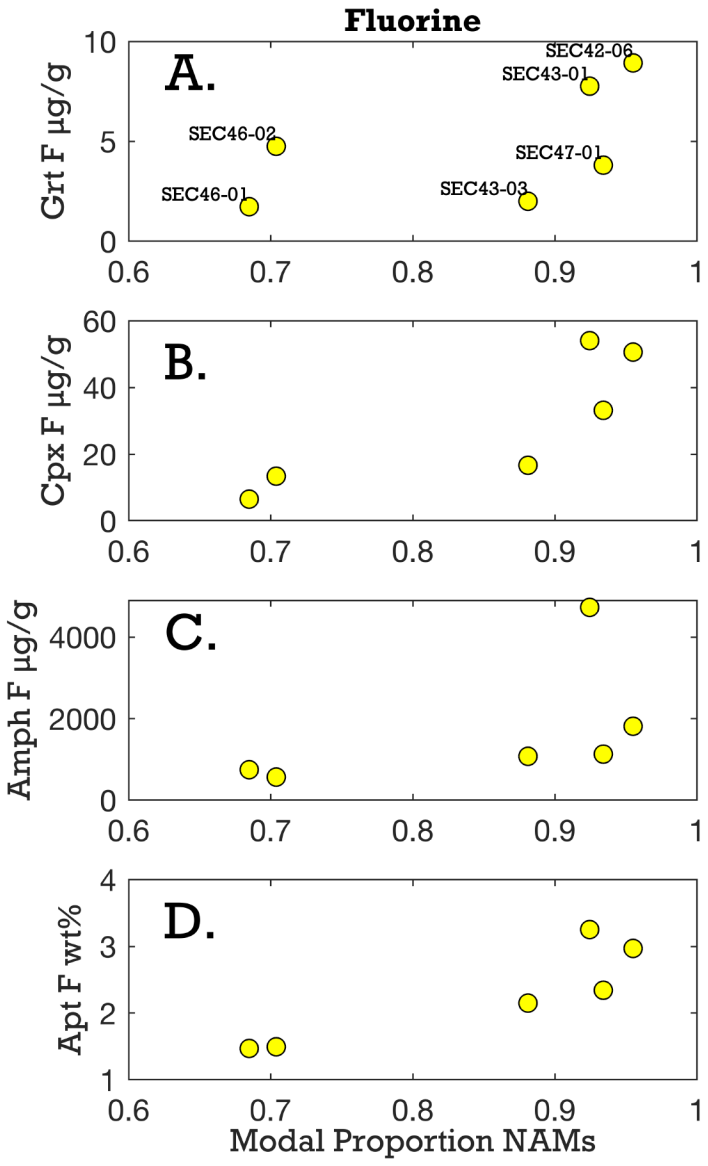

Supplemental Figure S8. Fluorine and chlorine concentrations in each phase as a function of the modal proportion of nominally anhydrous minerals (omphacite plus garnet). As the modal proportion of NAMs increases, so does the halogen concentration in most phases.

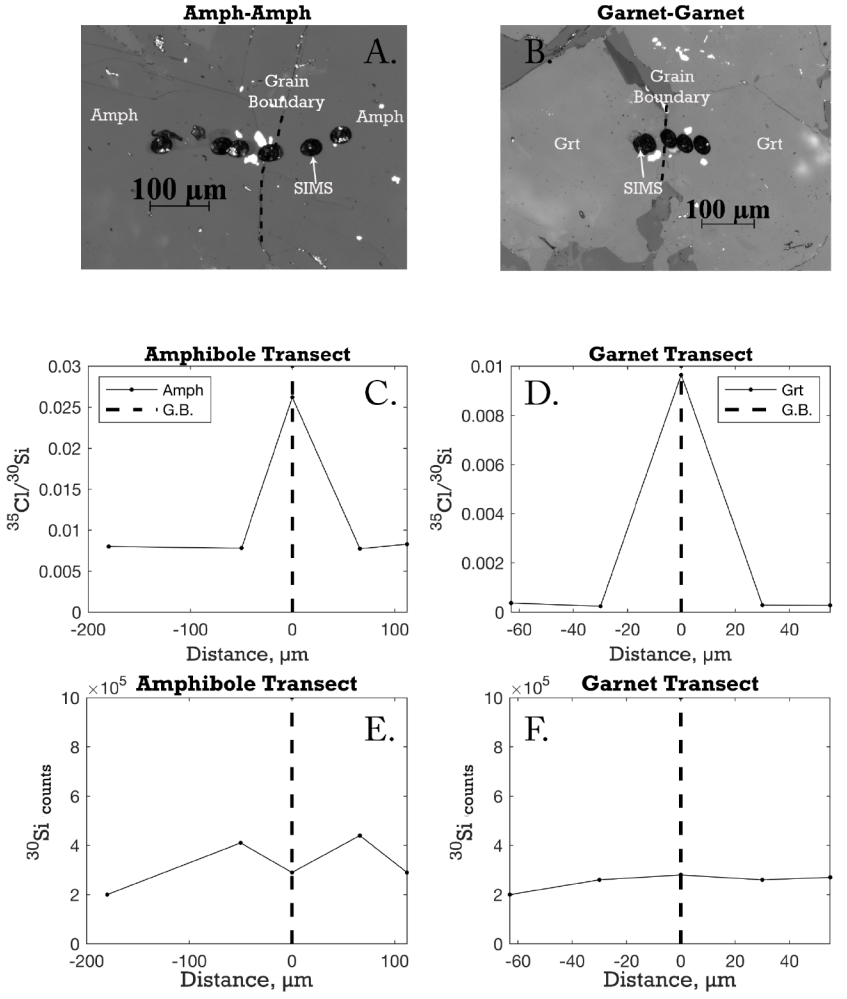

Supplemental Figure S9. Grain boundary transects using SIMS across amphibole (**a**) and garnet (**b**). While there are likely unaccounted for matrix effects with this approach, both measurements on the grain boundary qualitatively show pronounced spikes in Cl/Si ratios at near-constant constant Si counts, indicating Cl enrichment within the grain boundary (**c** and **d**). Also shown are raw ^{30}Si counts for comparison (**e** and **f**).